

Next-to-leading-order study of the associated production of $J/\psi + \gamma$ at the LHC

Rong Li^{1,3} and Jian-Xiong Wang^{2,3}¹*Department of Applied Physics, Xi'an Jiaotong University, Xi'an 710049, China*²*Institute of High Energy Physics, Chinese Academy of Sciences, P.O. Box 918(4), Beijing 100049, China*³*Theoretical Physics Center for Science Facilities, CAS, Beijing, 100049, China*

(Received 28 January 2014; published 16 June 2014)

The associate $J/\psi + \gamma$ production at the LHC is studied completely at next-to-leading order within the framework of nonrelativistic QCD. By using three sets of color-octet long-distance matrix elements obtained in previous prompt J/ψ studies, we find that only one of them can result in a positive transverse momentum (p_t) distribution of J/ψ production rate at the large p_t region. Based on reasonable consideration to cut down background, our estimation is measurable up to $p_t = 50$ GeV with the present data sample collected at 8 TeV LHC. All the color-octet long-distance matrix elements in J/ψ production could be fixed sensitively by including this proposed measurement and our calculation, and then a confident conclusion on the J/ψ polarization puzzle could be achieved.

DOI: [10.1103/PhysRevD.89.114018](https://doi.org/10.1103/PhysRevD.89.114018)

PACS numbers: 12.38.Bx, 13.25.Gv, 13.60.Le

Since the discovery of heavy quarkonium in the 1970s, the study on production and decay of J/ψ and Υ has played an important role in the research on the perturbative and nonperturbative aspects of QCD. In 1995, a new factorization framework, nonrelativistic QCD (NRQCD), was proposed to study the production and decay of heavy quarkonium [1]. It overcomes some shortcomings in the prevalent color-single model (CSM) [2] and makes the CSM be a part of it. By extracting the NRQCD long-distance matrix elements (LDMEs) from the matching between theoretical prediction and experimental data, the NRQCD calculation has given a good description on the transverse momentum distribution (p_t) of heavy quarkonium production at hadron colliders at leading order (LO) [3]. The phenomenological applications of the NRQCD have been investigated extensively [4], but the polarization of heavy quarkonium hadroproduction has been an open question for more than ten years.

The next-to-leading-order (NLO) QCD correction to the J/ψ inclusive hadroproduction in the CSM significantly enhanced the p_t distribution [5] and changed the polarization from transverse to longitudinal [6]. The later study including the contribution from the color-octet model (COM) parts ($^1S_0^8$ and $^3S_1^8$) at QCD NLO still cannot give a satisfactory prediction on the polarization of J/ψ [7]. In Ref. [8], the study on P-wave charmonium hadroproduction with the feed-down from χ_{cJ} to J/ψ had been obtained at QCD NLO. Soon after, the p_t distribution of the J/ψ production rate at full NLO QCD was given by two groups [9,10]. Then after two years, the p_t distributions on polarization for direct J/ψ hadroproduction at full NLO QCD were presented by two groups [11,12]. A few months later, a complete study [13] on the polarization of prompt J/ψ hadroproduction with the feed-down contribution from χ_{cJ} included was given, and it presents the first result

at QCD NLO that can be compared with the experimental measurements directly since all the polarization measurements are for prompt J/ψ . The recent measurements at the LHC by CMS [14] and LHCb [15] show disagreement with the prediction [13]. However, the results from the two groups [12,13] imply that the χ^2 fit to extract the LDMEs of J/ψ production is very sensitive to the input conditions due to the approximately linear correlation among the short-distance coefficients of the three color-octet parts, while the result from the group [11] has overcome the linear-correlation problem by including the measurement from photoproduction at the HERA at small J/ψ transverse momentum range. Therefore, no solid conclusion on the polarization of J/ψ could be achieved, and we await another relevant reliable perturbative prediction, which is experimentally measurable, and can break the linear correlation of the previous fit. Is the study on associate $J/\psi + \gamma$ hadroproduction at full QCD NLO a good candidate? Our study clearly indicates that it is a very good candidate with the present data sample collected at 8 TeV LHC.

Alternately, for Υ hadroproduction, there are studies on the p_t distribution of yield and polarization for the CS channel at QCD NLO [5,6] and at the partial next-to-next-to-leading order [16]. The NLO QCD correction to p_t distribution of the yield and polarization for $\Upsilon(1S, 3S)$ via S-wave CO states is presented in Ref. [17], and the NLO QCD correction to p_t distribution of the yield for $\Upsilon(1S)$ via all the CO states is presented in Ref. [18]. The complete NLO study on polarization of prompt Υ hadroproduction has been achieved in Ref. [19], which can explain the recent measurements on the polarization of $\Upsilon(1S, 2S, 3S)$ at the LHC by CMS Collaboration [20].

In addition to the study on the important inclusive heavy quarkonium hadroproduction, the study on the associate hadroproduction of heavy quarkonium and photon

(or W^\pm , Z^0 bosons) was proposed as a supplemental channel to probe the gluon content in the proton [21] or to investigate the production mechanism of heavy quarkonium [22]. The NLO QCD correction to $J/\psi + W^\pm (Z^0)$ had been calculated in Ref. [23]. Our study [24] shows the NLO QCD correction to the associate $J/\psi + \gamma$ hadroproduction in the CSM significantly enhanced the p_t distribution in the high-momentum region and changed the polarization from transverse to longitudinal. The relevant study [25] can reproduce our results in a partial NLO calculation. Recently some colleagues proposed to investigate the transverse dynamics and polarization of gluon in proton by using the inclusive hadroproduction of $\Upsilon + \gamma$ [26]. To obtain an experimentally measurable observable at full QCD NLO, we present the study on associate $J/\psi + \gamma$ hadroproduction at the NLO with full COM contribution in this work.

In the NRQCD framework, the inclusive production of $J/\psi + \gamma$ can be factorized as

$$\begin{aligned} \sigma(p + \bar{p} \rightarrow J/\psi + \gamma + X) \\ = \sum_{i,j} \int dx_1 dx_2 G_p^i(x_1) G_{\bar{p}}^j(x_2) \hat{\sigma}(ij \rightarrow (Q\bar{Q})_n \\ + \gamma + X) \langle O_n^{J/\psi} \rangle. \end{aligned} \quad (1)$$

Here $G_{p(\bar{p})}^{i(j)}$ are the parton distribution functions(PDFs), $\hat{\sigma}$ presents the parton level cross section, and $\langle O_n^{J/\psi} \rangle$ are the LDMEs. The relevant parton level processes are listed as follows:

$$g + g \rightarrow Q\bar{Q}[^3S_1^1, ^1S_0^8, ^3S_1^8, ^3P_J^8] + \gamma, \quad (2)$$

$$g + g \rightarrow Q\bar{Q}[^3S_1^1, ^1S_0^8, ^3S_1^8, ^3P_J^8] + \gamma + g, \quad (3)$$

$$q + \bar{q} \rightarrow Q\bar{Q}[^3S_1^1, ^1S_0^8, ^3S_1^8, ^3P_J^8] + \gamma, \quad (4)$$

$$q + \bar{q} \rightarrow Q\bar{Q}[^1S_0^8, ^3S_1^8, ^3P_J^8] + \gamma + g, \quad (5)$$

$$q(\bar{q}) + g \rightarrow Q\bar{Q}[^3S_1^1, ^1S_0^8, ^3S_1^8, ^3P_J^8] + \gamma + q(\bar{q}). \quad (6)$$

In addition to the $p_t(J/\psi)$ distribution of the $J/\psi + \gamma$ hadroproduction at QCD NLO, the related polarization observable α of J/ψ is also studied. α is measured by using the angular distribution of the decayed lepton pair in helicity frame and related to the spin density matrix of J/ψ as

$$\alpha(p_t) = \frac{d\sigma_{11}/dp_t - d\sigma_{00}/dp_t}{d\sigma_{11}/dp_t + d\sigma_{00}/dp_t}. \quad (7)$$

Here the “1” and “0” mean the transverse and longitudinal polarization of J/ψ at the matrix element level. The calculations of the spin density matrix for the

$Q\bar{Q}[^3S_1^1, ^3S_1^8, ^1S_0^8]$ are the same as what has been done in other similar processes [7].

In handling the processes in the COM, there are two aspects that are different from the color-singlet case. The first is that in process (6), γ can be collinear with quark or antiquark $q(\bar{q})$ in final states in some region of the phase space. This infrared divergence will cancel the infrared divergence in the QED correction of $pp \rightarrow J/\psi + g$. Because we observe the photon in the final states, it means that we have to impose a cut on this process to isolate a photon from the quark jet [27],

$$p_t^i \leq p_t^\gamma \frac{1 - \cos R_{\gamma i}}{1 - \cos \delta_0} \quad \text{for } R_{\gamma i} < \delta_0. \quad (8)$$

The definitions of the p_t^i , p_t^γ , $\cos R_{\gamma i}$, and the δ_0 can be found in Ref. [27]. Here we set $\delta_0 = 0.7$. For the consideration on the experimental measurement, we also set the cutoff on the transverse momentum of the photon(p_t^γ). Therefore, the numerical results will rely heavily on this condition. The second aspect that is different from the color-singlet case is that the color-octet P-wave parts have additional infrared divergence, which will be factorized into the LDMEs by using the same method as in Ref. [28]. In the calculation of real process $Q\bar{Q}[^3P_J^8] + \gamma + g$ hadroproduction, there is a soft divergence related to $Q\bar{Q}$ pair radiating the soft gluon and it can be factorized as an amplitude square of $Q\bar{Q}[^3S_1^8, ^3S_1^1] + \gamma$ hadroproduction times a soft factor that contains soft divergence. This divergence can be absorbed into the redefinition of the $Q\bar{Q}[^3S_1^8, ^3S_1^1]$ LDMEs at NLO, and there are finite parts being left. Therefore, in addition to the direct calculation of the $Q\bar{Q}[^3P_J^8]$ state, we also have to take into account the contribution from the left parts, which we call the q-term parts.

After generating the FORTRAN codes of these processes individually by using the Feynman diagram calculation (FDC) package [29], we check the cancelation of infrared and ultraviolet divergence, the gauge invariance, and the cut independence, respectively. Because of the complexity of the analytic expressions, we use the quadruple precision program in some of the calculations to avoid the numerical instability.

To obtain the numerical results, we choose the following parameters and cut conditions. The charm quark mass m_c is set as 1.5 GeV and will vary from 1.4 to 1.6 GeV to estimate the related uncertainty. The renormalization and factorization scales are set to $\mu_r = \mu_f = \mu_0 = \sqrt{(2m_c)^2 + p_t^2}$ and will vary from $\mu_0/2$ to $2\mu_0$ to estimate the uncertainties. The NRQCD scale μ_Λ is chosen as m_c . As for the experimental conditions, we use $\sqrt{s} = 7, 8, 14$ TeV at the LHC, the rapidity cuts $|y_{J/\psi, \gamma}| \leq 3$, or pseudorapidity cut $|\eta_\gamma| \leq 1.45$ and $p_t^i < 1.5, 3, 5, 15$ GeV cuts. The fine structure constant is chosen as $\frac{1}{128}$. The CTEQ6L1 and the CTEQ6M PDFs and the corresponding α_s running formula are used to calculate the LO and the NLO numerical results [30].

The involved LDMEs were extracted at the NLO by different groups with different considerations [10,12,13,31]. In Ref. [32] the authors investigated these LDME sets and concluded that the universality of LDMEs is challenged. The two LDME sets in Refs. [10,12] are from the same group, and we use their former results on the combination of LDMEs in Ref. [10] to estimate the numerical results since the feed-down contribution from χ_c and ψ' have been considered there, which could affect the theoretical prediction significantly as discussed in Ref. [13]. We list these LDME sets in Table I. For the LDMEs in Ref. [10], only the combinations of them, $M_{0,r_0}^{J/\psi}$ and $M_{1,r_1}^{J/\psi}$, are given as

$$M_{0,r_0}^{J/\psi} = \langle O^{J/\psi}(^1S_0^8) \rangle + \frac{r_0}{m_c^2} \langle O^{J/\psi}(^3P_0^8) \rangle, \quad (9)$$

$$M_{1,r_1}^{J/\psi} = \langle O^{J/\psi}(^3S_1^8) \rangle + \frac{r_1}{m_c^2} \langle O^{J/\psi}(^3P_0^8) \rangle, \quad (10)$$

where $r_0 = 3.9$, $r_1 = -0.56$, $M_{0,r_0}^{J/\psi} = 0.074$, and $M_{1,r_1}^{J/\psi} = 0.0005$. With requiring the LDMEs to be positive we set the three individual color-octet LDMEs from the above combinations under two conditions in Table I, which we will refer to as ‘‘Ma extension’’ in the following parts.

It is shown in Fig. 1 that the color-octet $^3P_J^8$ state, just like $^3S_1^8$ and $^1S_0^8$ state, gives a positive short-distance coefficient in all p_t regions in contrast to the J/ψ inclusive hadroproduction at QCD NLO case, where the color-octet $^3P_J^8$ state gives a negative short-distance coefficient in the large p_t region. The difference makes the p_t distribution of $J/\psi + \gamma$ production rate an observable that can break the linear correlation in the previous fit without including the small p_t range data from the measurement at the HERA.

The first column of Fig. 2 presents the results at $\sqrt{s} = 7$ TeV. In order to investigate the dependence on p_t^γ cut, we plot the p_t distribution of production rate and polarization observable α with different p_t^γ cuts and two sets of the LDMEs in Ma extension. The plots show that the dependence on p_t^γ cut decreases with the increase of $p_t(J/\psi)$ and different p_t^γ cuts make the p_t distribution shift parallel in contrast to the color-singlet channel in Ref. [24],

TABLE I. The NRQCD LDMEs $\langle O^{J/\psi}(n) \rangle$ extracted by three groups in Refs. [10,12,13,31] at the NLO with $\langle O^{J/\psi}(^3S_1^8) \rangle = 1.32$ (1.16) GeV^3 used in Ref. [31] (in the others). The NRQCD LDMEs in Ma extension1 and extension2 are determined from the combination extracted in Ref. [10].

n	$^1S_0^8, \text{GeV}^3$	$^3S_1^8, \text{GeV}^3$	$^3P_0^8, \text{GeV}^5$
Butenschoen [31]	0.0497	0.0022	-0.0161
Gong [13]	0.097	-0.0046	-0.0214
Chao [12]	0.089	0.0030	0.0126
Ma extension1	0.074	0.0005	0
Ma extension2	0	0.011	0.019

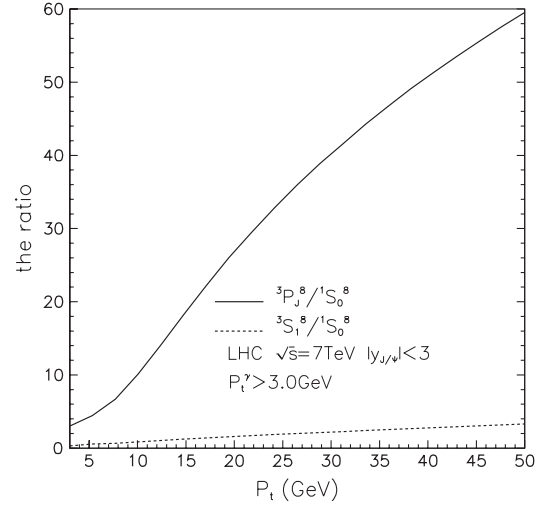


FIG. 1. The ratio of $d\sigma(^3P_J^8)/d\sigma(^1S_0^8)$ and $d\sigma(^3S_1^8)/d\sigma(^1S_0^8)$ as functions of p_t .

where the p_t distribution of J/ψ production rate and α are insensitive to the p_t^γ cut in the same p_t region. The reason is that the $^3P_J^8$ and $^1S_0^8$ channels in the COM are sensitive to the cuts.

In the second column in Fig. 2, we give results at $\sqrt{s} = 14$ TeV. The shaded band represents the uncertainties estimated by varying the m_c , the renormalization scale μ_r and factorization scale μ_f . The plots show that the uncertainties of production rate become larger and that of α become smaller as p_t increasing. The COM contribution on production rate dominant over that of CSM and are about 2 orders larger than the color-singlet ones at $p_t = 50$ GeV. We also plot the p_t distribution with the LDME sets in Refs. [31] and [13], the value of the numerical results are negative in the p_t distribution of production rate when $p_t > 13$ GeV, and α s in both cases are out of the physical region when $p_t > 10$ GeV.

From the results at the first and second columns of Fig. 2, we know that the p_t distribution of $J/\psi + \gamma$ hadroproduction rate is a good observable to distinguish different LDME sets. Is it measurable or not at the 8 GeV LHC with present 23 fb^{-1} integrated luminosity? To suppress the background efficiently, the $p_t^\gamma > 15$ GeV cut on photon is applied, together with $|y_{J/\psi}| < 2.4$ and $|\eta_\gamma| < 1.45$ for photon reconstruction efficiency consideration. The plots in the third column of Fig. 2 show that the p_t distributions of the J/ψ production rate in the COM with Ma extension LDME sets are about 10(100) times larger than that in the CSM. The other two LDME sets give the positive predictions in lower p_t region and negative ones when p_t is larger than 31 GeV. When p_t is larger than 20 GeV, the results show many differences on the J/ψ polarization predictions α with the CSM (COM) mechanism and three LDME sets. It is worth mentioning that only real processes at QCD NLO contribute when $p_t^{J/\psi} < 15$ GeV in the third column case with $p_t^\gamma > 15$ GeV.

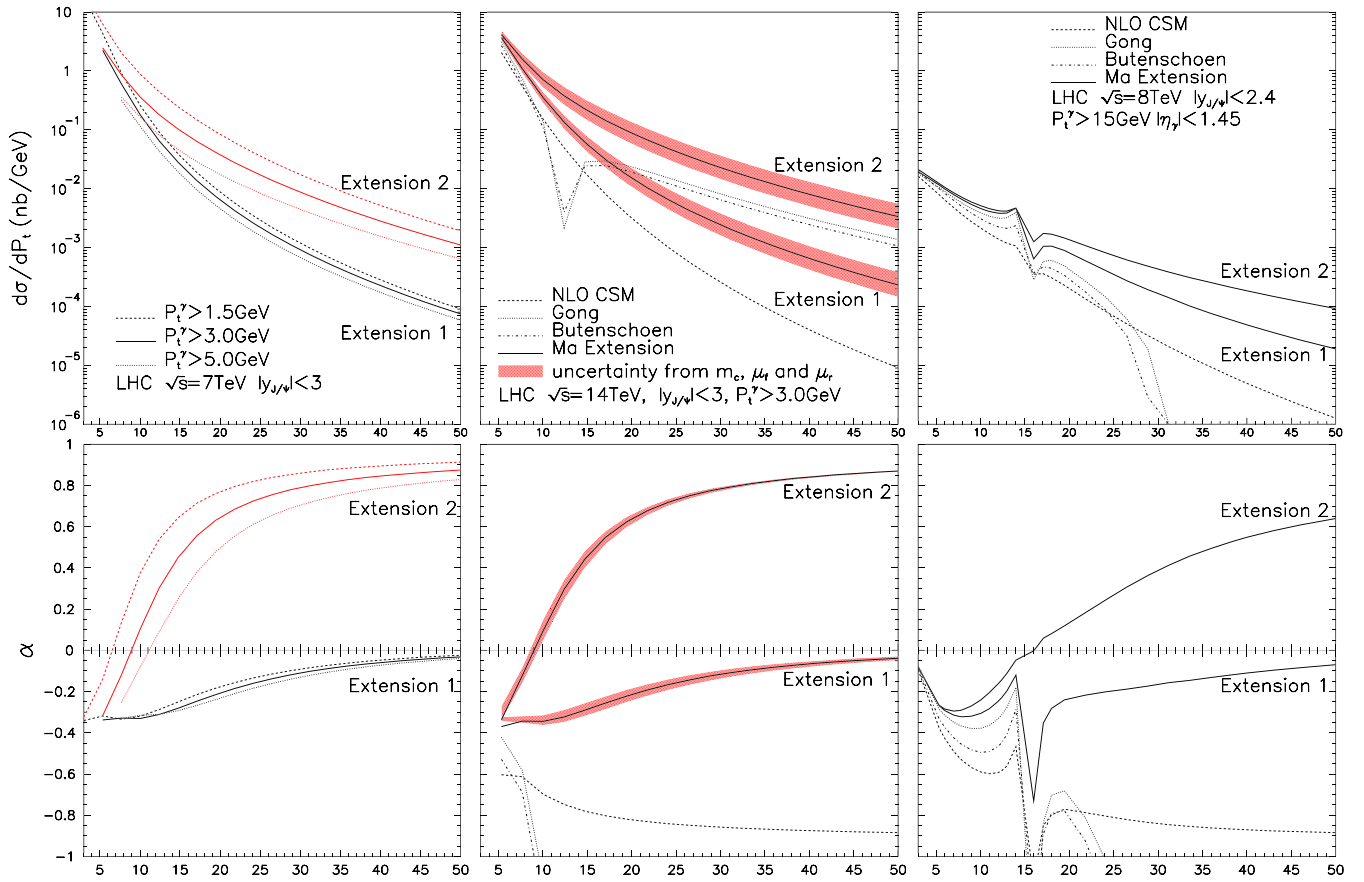


FIG. 2 (color online). The $p_t(J/\psi)$ distributions for $J/\psi + \gamma$ production (upper parts) and polarization (lower parts) with different conditions. Figures in the same column are of the same conditions and line types. The shaded band in the second column represent the uncertainty from variation of μ_f & μ_r and m_c . The third column shows results with $p_t^\gamma > 15$ GeV and different LDME sets.

In summary, we present the study on associate $J/\psi + \gamma$ hadroproduction at the NLO with full COM contribution at the LHC. Our numerical results show that the contribution from color-octet channels enhances the differential cross section about 2 order in the large p_t region. As for the J/ψ polarization, the color-octet contribution changes it from longitudinal one to transverse one. From all the plots in Fig. 2, it is manifest that the most important uncertainty comes from the variation of LDMEs. The LDME sets of Butenschoen and Gong lead to the unphysical p_t distribution of production rate (negative) and polarization observable α (out of range -1 to 1) at large p_t range, while the LDME set of Ma extension gives physical ones at all the p_t range. Even within Ma extension, the p_t distributions of production rate are of huge difference (10 times at $p_t = 50$ GeV) between the extension2 and extension1. The polarization observable α changes from slightly longitudinal in extension1 to the transverse in extension2.

In conclusion, the theoretical predictions are sensitive to the LDMEs heavily and can break the linear correlation in previous fit without small p_t range measurement. To obtain an experimentally measurable observable at the 8 GeV LHC with present 23 fb^{-1} integrated luminosity, $p_t^\gamma > 15$ GeV

cut on the observed photon is applied to efficiently suppress the background and $|\eta_\gamma| < 1.45$ is used. With these conditions, the photon reconstruction efficiency is larger than 0.7 [33], and we use 0.7 in the following estimation, $\text{Br}(J/\psi \rightarrow \mu^+ + \mu^-) = 0.06$, which is also used to represent reconstruction of J/ψ from the observed $\mu^+ + \mu^-$ pair. Then the plots in the third column of Fig. 2 indicate that $960 \sim 1920$ events at $p_t = 17$ GeV and $19 \sim 96$ events at $p_t = 50$ GeV could be reconstructed from the sample data. Therefore, the p_t distribution of production rate is experimentally measurable with the present data sample collected at 8 TeV LHC. All the color-octet LDMEs in J/ψ production could be fixed sensitively by including this proposed measurement and our calculation.

ACKNOWLEDGMENTS

We thank Dr. Bin Gong, Hong-Fei zhang, and Lu-Ping Wan for helpful discussions. R.L. also thanks Qiang Li for the discussion on the isolation of photon. This work is supported by the National Natural Science Foundation of China (Grants No. 11105152, No. 10935012, and No. 11005137), DFG and NSFC (CRC110), and by CAS under Project No. INFO-115-B01.

- [1] G. T. Bodwin, E. Braaten, and G. P. Lepage, *Phys. Rev. D* **51**, 1125 (1995); **55**, 5853(E) (1997).
- [2] M. B. Einhorn and S. D. Ellis, *Phys. Rev. D* **12**, 2007 (1975); S. D. Ellis, M. B. Einhorn, and C. Quigg, *Phys. Rev. Lett.* **36**, 1263 (1976); C.-H. Chang, *Nucl. Phys.* **B172**, 425 (1980); E. L. Berger and D. L. Jones, *Phys. Rev. D* **23**, 1521 (1981); R. Baier and R. Ruckl, *Nucl. Phys.* **B201**, 1 (1982).
- [3] P. L. Cho and A. K. Leibovich, *Phys. Rev. D* **53**, 150 (1996); **53**, 6203 (1996).
- [4] N. Brambilla *et al.* (Quarkonium Working Group Collaboration), arXiv:hep-ph/0412158; J. P. Lansberg, *Int. J. Mod. Phys. A* **21**, 3857 (2006).
- [5] J. M. Campbell, F. Maltoni, and F. Tramontano, *Phys. Rev. Lett.* **98**, 252002 (2007).
- [6] B. Gong and J.-X. Wang, *Phys. Rev. Lett.* **100**, 232001 (2008); B. Gong and J.-X. Wang, *Phys. Rev. D* **78**, 074011 (2008).
- [7] B. Gong, X. Q. Li, and J.-X. Wang, *Phys. Lett. B* **673**, 197 (2009); **693**, 612(E) (2010).
- [8] Y.-Q. Ma, K. Wang, and K.-T. Chao, *Phys. Rev. D* **83**, 111503 (2011).
- [9] M. Butenschoen and B. A. Kniehl, *Phys. Rev. Lett.* **106**, 022003 (2011).
- [10] Y.-Q. Ma, K. Wang, and K.-T. Chao, *Phys. Rev. Lett.* **106**, 042002 (2011).
- [11] M. Butenschoen and B. A. Kniehl, *Phys. Rev. Lett.* **108**, 172002 (2012).
- [12] K.-T. Chao, Y.-Q. Ma, H.-S. Shao, K. Wang, and Y.-J. Zhang, *Phys. Rev. Lett.* **108**, 242004 (2012).
- [13] B. Gong, L.-P. Wan, J.-X. Wang, and H.-F. Zhang, *Phys. Rev. Lett.* **110**, 042002 (2013).
- [14] S. Chatrchyan *et al.* (CMS Collaboration), *Phys. Lett. B* **727**, 381 (2013).
- [15] R. Aaij *et al.* (LHCb Collaboration), *Eur. Phys. J. C* **73**, 2631 (2013).
- [16] P. Artoisenet, J. M. Campbell, J. P. Lansberg, F. Maltoni, and F. Tramontano, *Phys. Rev. Lett.* **101**, 152001 (2008).
- [17] B. Gong, J.-X. Wang, and H.-F. Zhang, *Phys. Rev. D* **83**, 114021 (2011).
- [18] K. Wang, Y.-Q. Ma, and K.-T. Chao, *Phys. Rev. D* **85**, 114003 (2012).
- [19] B. Gong, L.-P. Wan, J.-X. Wang, and H.-F. Zhang, *Phys. Rev. Lett.* **112**, 032001 (2014).
- [20] S. Chatrchyan *et al.* (CMS Collaboration), *Phys. Rev. Lett.* **110**, 081802 (2013).
- [21] M. Drees and C. S. Kim, *Z. Phys. C* **53**, 673 (1992); M. A. Doncheski and C. S. Kim, *Phys. Rev. D* **49**, 4463 (1994).
- [22] C. S. Kim and E. Mirkes, *Phys. Rev. D* **51**, 3340 (1995); E. Mirkes and C. S. Kim, *Phys. Lett. B* **346**, 124 (1995); D. P. Roy and K. Sridhar, *Phys. Lett. B* **341**, 413 (1995); C. S. Kim, J. Lee, and H. S. Song, *Phys. Rev. D* **55**, 5429 (1997); P. Mathews, K. Sridhar, and R. Basu, *Phys. Rev. D* **60**, 014009 (1999); B. A. Kniehl, C. P. Palisoc, and L. Zwierner, *Phys. Rev. D* **66**, 114002 (2002); J. P. Lansberg and C. Lorce, *Phys. Lett. B* **726**, 218 (2013).
- [23] G. Li, M. Song, R.-Y. Zhang, and W.-G. Ma, *Phys. Rev. D* **83**, 014001 (2011); S. Mao, M. Wen-Gan, L. Gang, Z. Ren-You, and G. Lei, *J. High Energy Phys.* **02** (2011) 071; **12** (2012) 010(E); B. Gong, J.-P. Lansberg, C. Lorce, and J. Wang, *J. High Energy Phys.* **03** (2013) 115.
- [24] R. Li and J.-X. Wang, *Phys. Lett. B* **672**, 51 (2009).
- [25] J. P. Lansberg, *Phys. Lett. B* **679**, 340 (2009).
- [26] W. J. den Dunnen, J.-P. Lansberg, C. Pisano, and M. Schlegel, *Phys. Rev. Lett.* **112**, 212001 (2014).
- [27] S. Frixione, *Phys. Lett. B* **429**, 369 (1998).
- [28] J.-X. Wang and H.-F. Zhang, *Phys. Rev. D* **86**, 074012 (2012).
- [29] J.-X. Wang, *Nucl. Instrum. Methods Phys. Res., Sect. A* **534**, 241 (2004).
- [30] J. Pumplin, D. R. Stump, J. Huston, H. L. Lai, P. M. Nadolsky, and W. K. Tung, *J. High Energy Phys.* **07** (2002) 012.
- [31] M. Butenschoen and B. A. Kniehl, *Phys. Rev. D* **84**, 051501 (2011).
- [32] M. Butenschoen and B. A. Kniehl, *Mod. Phys. Lett. A* **28**, 1350027 (2013).
- [33] CMS Collaboration, CMS-DP-2013-010.